JAAS

Accepted Manuscript

This is an *Accepted Manuscript*, which has been through the Royal Society of Chemistry peer review process and has been accepted for publication.

Accepted Manuscripts are published online shortly after acceptance, before technical editing, formatting and proof reading. Using this free service, authors can make their results available to the community, in citable form, before we publish the edited article. We will replace this *Accepted Manuscript* with the edited and formatted *Advance Article* as soon as it is available.

You can find more information about *Accepted Manuscripts* in the Information for Authors.

Please note that technical editing may introduce minor changes to the text and/or graphics, which may alter content. The journal's standard Terms & Conditions and the Ethical guidelines still apply. In no event shall the Royal Society of Chemistry be held responsible for any errors or omissions in this *Accepted Manuscript* or any consequences arising from the use of any information it contains.

ROYAL SOCIETY OF CHEMISTRY

www.rsc.org/jaas

Laser ablation – tandem ICP – mass spectrometry (LA-ICP-MS/MS) for direct Sr isotopic analysis of solid samples with high Rb/Sr ratio

Eduardo Bolea-Fernandez[a*], Stijn J.M. Van Malderen[a*], Lieve Balcaen[a], Martín Resano[b] and Frank Vanhaecke[a,**]

[a]Ghent University, Department of Analytical Chemistry, Krijgslaan 281-S12, 9000 Ghent, Belgium

[b]University of Zaragoza, Aragón Institute of Engineering Research (I3A), Department of Analytical Chemistry, Pedro Cerbuna 12, 50009 Zaragoza, Spain

[*]Both authors contributed equally to this work

[**]Corresponding author

ABSTRACT

The combination of laser ablation and tandem ICP – mass spectrometry (LA-ICP-MS/MS) allows for successful Sr isotopic analysis of solid samples with high Rb/Sr ratio. Isobaric overlap at a mass-to-charge ratio of 87 (^{87}Sr – ^{87}Rb) is overcome *via* chemical resolution. By using CH_3F/He (10% CH_3F in He), in an octopole collision-reaction cell, Sr^+ ions are converted into the corresponding SrF^+ reaction product ions, while Rb^+ ions show no reactivity towards this gas mixture. Two sample introduction setups, leading to "dry" and "wet" plasma conditions, respectively, were evaluated and the figures of merit documented in detail. The ^{87}Sr/^{86}Sr isotope ratio results were corrected for instrumental mass discrimination using a double correction approach – internal correction using the Russell law, followed by external correction in a sample-standard bracketing (SSB) approach. NIST SRM 610 was applied as external standard for mass bias correction; no closer matrix-matching was required for the sample types investigated. Under "wet" plasma conditions, accurate and precise (0.02 – 0.05 % RSD) ^{87}Sr/^{86}Sr isotope ratio results were obtained for 7 glass-type geological reference materials.

1. INTRODUCTION

Strontium (Sr) isotopic analysis is a key tool for obtaining relevant information in many application areas – e.g., geochronological dating (Rb/Sr dating), obtaining other types of geochemical information, provenancing of, among other, agricultural products and archaeological objects, and animal and human migration studies.[1]

Accurate and precise determination of the isotopic composition of Sr *via* ICP-mass spectrometry is not self-evident, despite of the relatively more pronounced natural variation in its isotopic composition (coming from the radiogenic character of ^{87}Sr, i.e., β^- decay of ^{87}Rb into ^{87}Sr with a half-life $T_{1/2}$ of $4.88 \cdot 10^{10}$ years[2]),[3] in comparison to elements that only display natural variation as a result of isotope fractionation.[4] In fact, Sr is one of the only elements for which thermal ionization mass spectrometry (TIMS)[5] is preferred over multi-collector ICP-MS, as a result of the occurrence of spectral interference with the latter.[6] Besides the isobaric overlap of ^{87}Sr and ^{87}Rb at a mass-to-charge (m/z) ratio of 87,[7] the contamination of Ar with Kr will also induce isobaric overlap at m/z ratios 84 and 86. However, due to the increased sample throughput of MC-ICP-MS, the latter technique is gaining ground, compared to TIMS.[8] For the less demanding applications, also single-collector ICP-MS has been successfully used in this context.[9-11] In ICP-MS, pneumatic nebulization (PN) is the standard sample introduction system, although its use is limited to liquid or digested samples, while prior chemical separation of Sr and Rb is a must, and remaining Rb and Kr contamination of the Ar plasma gas need to be corrected for.[12] Laser ablation (LA) can be seen as an attractive alternative for this kind of analysis owing to the absence of sample preparation, minimal sample damage, efficient sample introduction, high sample throughput and the ability to perform spatially resolved analysis of selected sample regions.[13-16] However, Sr isotopic analysis by means of LA-ICP-MS is far from evident given the spectral interferences mentioned above.[17, 18]

Several approaches have been deployed to avoid or mitigate isobaric interference from ^{87}Rb and other spectral interferences (e.g., from Kr^+ and the polyatomic ions $ArCa^+$ and/or Ca_2^+) affecting the measurement of the Sr isotopes.[19] Chemical isolation of Sr from the concomitant matrix elements can be regarded as the standard approach to overcome the spectral interferences in the isotopic analysis of

Sr *via* PN-ICP-MS and it is considered imperative for samples with high Rb/Sr ratio.[20-22] However, this approach is laborious and time-consuming, thus reducing sample throughput and increasing the risk of contamination. Moreover, the analysis of solid samples requires digestion, involving the use of concentrated mineral acids.

The use of high mass resolution (HR) in ICP-MS instrumentation equipped with a double-focusing sector field mass spectrometer is a powerful way to cope with spectral overlap,[23, 24] but, the maximum resolution attained by present-day commercially available instrumentation is limited to 10,000, which is by far insufficient to resolve the isobaric overlap of the signals of ^{87}Sr and ^{87}Rb ($R_{required}$ ~300,000),[25] thus limiting the applicability of LA-HR-ICP-MS to samples with a sufficiently low Rb/Sr ratio ≤ 0.2.[26-28] Even in those cases where the Rb/Sr ratio is low, both for PN-HR-ICP-MS (even after chemical Sr/Rb separation) and for LA-HR-ICP-MS, mathematical correction is required for the (remaining) Rb and the other spectral interferences mentioned above.[29, 30]

Also the use of a collision-reaction cell in quadrupole-based ICP-MS (ICP-QMS) is an elegant approach for overcoming spectral overlap and compared to HR-ICP-MS instrumentation, ICP-QMS still offers higher robustness at a lower purchase and maintenance cost. Several works to date have reported on the use of ICP-QMS for isotope ratio determination, mainly for the study of induced changes in the isotopic composition in the context of tracer experiments or elemental assay *via* isotope dilution mass spectrometry (IDMS),[31] but also for elements displaying a relatively large natural variation in their isotopic pattern (e.g., Li, B, Pb, Sr).[11, 32, 33] In modern ICP-QMS, equipped with a collison/reaction cell, isobaric overlap can be resolved *via* chemical resolution, by pressurizing the cell with a selective reactive gas that reacts differently with the interfering ion and the analyte ion, forming new reaction product ions and allowing interference-free determination.[34, 35] However, the number of works reporting on the use of ICP-QMS and LA-ICP-QMS using chemical resolution for interference-free isotopic analysis of elements suffering from strong spectral overlap is thus far very limited,[36] and no works to date have reported on their use for direct Sr isotopic analysis of solid samples with high Rb/Sr ratio. This might be attributed to the occurrence of new spectral interferences due to uncontrolled reactions in the cell, strong matrix effects, and the requirement of matrix-matching for mass bias correction.[37-39]

Recently (2012), a tandem ICP-MS device (ICP-MS/MS) has been introduced onto the market. This novel set-up allows for a better control of the reactions in the cell by removing all concomitant elements with a mass-to-charge (m/z) ratio that differs from that of the analyte ion by means of an additional quadrupole located before an octopole collision-reaction cell. After chemical reaction in the cell, the analyte ion can be measured interference-free at the original m/z ratio (conversion of the interfering ion) or at a different m/z ratio as a new reaction product ion *via* the use of a second quadrupole.[40] ICP-MS/MS with methyl fluoride (CH_3F) as reaction gas has been successfully applied to the interference-free determination of ultra-trace concentrations of several elements (e.g., transition metals, As, Se),[41, 42] and more recently, for accurate and precise (0.05 % RSD) Sr isotopic analysis of digested geological materials.[43] However, despite of the inherent benefits of tandem ICP-MS to avoid spectral overlap and the fast increase in the number of publications for elemental [44-46] and isotopic [47-50] analysis, only a few works to date have reported on the use of LA-ICP-MS/MS,[51] and according to the best of the authors' knowledge, no publications thus far have described the use of LA-ICP-MS/MS for isotopic analysis.

This work explores the capabilities of LA-ICP-MS/MS for Sr isotopic analysis, with the aim of obtaining direct isotopic information from solid samples with high (i.e., also > 0.2) Rb/Sr ratio.

2. EXPERIMENTAL

2.1. *Instrumentation*

An Analyte G2 (Teledyne CETAC Technologies, Omaha, USA) 193 nm ArF*excimer-based LA-unit, equipped with a HELEX 2 ablation cell, coupled to an Agilent 8800 tandem ICP-MS instrument (ICP-QQQ, Agilent Technologies, Japan) was used for all measurements. Two different sample introduction configurations, aimed at obtaining "dry" and "wet" plasma conditions, respectively, were evaluated. For "dry" plasma conditions, a standard LA-ICP-MS configuration was used. He was used as carrier gas, and Ar was added as a make-up gas downstream *via* a glass mixing bulb between the ablation cell and the ICP torch. For "wet" plasma conditions, a Peltier-cooled Scott-type spray chamber (2°C) was inserted for the simultaneous introduction (*via* two different inlets) of the LA aerosol – previously mixed with Ar make-up gas in the glass mixing bulb – and milli-Q water aerosol, produced using a

MicroMist nebulizer (400 µL min^{-1}). All connections were realized with 2 mm internal diameter PTFE tubing. See Figure 1 for a detailed graphical representation of both approaches.

The octopole collision-reaction cell was pressurized with a mixture of CH_3F/He (1:9, Air Liquide, Belgium), introduced in a flow rate range of 0 - 1 mL min^{-1} (mass flow controller calibrated for O_2).

2.2. *Samples and standards*

2.2.1. *Standards and reagents*

The following standard reference materials (SRMs), available from NIST (National Institute of Standards and Technology, MD, USA), were selected for method development and mass bias correction purposes: SRM 610 and SRM 612 (trace elements in a glass matrix).[52, 53]

For "wet" plasma conditions, ultra-pure water (resistivity ≥ 18.2 MΩ cm) provided by a Milli Q Element water purification system (Millipore, France) was used.

2.2.2. *Samples*

7 geological reference materials (RMs) – MPI-DING (Max-Planck-Institut für Chemie, Germany) ATHO-G "rhyolite glass", MPI-DING T1-G "diorite glass", USGS (United States Geological Survey, VA, USA) BCR-2G "basalt glass", USGS BHVO-2G "basalt glass", USGS GSD-1G "basalt glass", USGS NKT-1G "nephelinite glass" and USGS TB-1G "basalt glass" were analyzed for their Sr isotopic composition. The selection was carried out in order to cover a wide range of $^{87}Sr/^{86}Sr$ isotope ratios, Sr concentrations and Rb/Sr ratios (see Table 1). The Rb/Sr ratios in the (MPI-DING, NIST and USGS) RMs used display a range from 0.02 to 0.82, the latter being considerably higher than the 0.2 maximum limit cited in earlier work. From the http://earthref.org/GERMRD[54] website, which summarizes data on the geochemistry of all reservoirs in the Earth, it can be seen that a Rb/Sr ratio > 1 is exceptional. The results were compared to preferred and/or compiled GeoReM reference values for validation.[53]

2.3. *Procedure for Sr isotopic analysis via LA-ICP-MS/MS*

The instrument settings and data acquisition parameters used for Sr isotopic analysis *via* LA-ICP-MS/MS using both approaches i.e., under "dry" and "wet" plasma conditions, are summarized in Table 2.

Prior to analysis, all RMs were embedded into epoxy resin (bisphenol A diglycidyl ether, Streurs, Denmark) and subsequently polished mechanically with SiC paper (P1200 to P4000) and colloidal silica suspension (40 nm grain size) to remove any surface feature.

NIST SRMs 610 and 612 were selected as the external standards for mass discrimination correction purposes. Each sample was analyzed 5 consecutive times in a standard-sample-standard sequence, corresponding to 6 and 5 analyses for standard and sample, respectively. 12 replicate measurements (line scans) were performed during each analysis. The raw ratios thus obtained were corrected for mass bias[55] using the double correction approach, consisting of internal correction assuming a constant $^{88}Sr/^{86}Sr$ isotope ratio (Russell law – equation 1), followed by sample-standard bracketing (SSB – equation 2).

$$R_{sample,corrected}^{^{87}Sr/^{86}Sr} = R_{sample,measured}^{^{87}Sr/^{86}Sr} \; x \left(\frac{m_{^{87}Sr}}{m_{^{86}Sr}}\right)^{f} \; ; \; f = \ln\left[\frac{R_{true}^{^{88}Sr/^{86}Sr}}{R_{measured}^{^{88}Sr/^{86}Sr}}\right] \Big/ \ln\left[\frac{m_{^{88}Sr}}{m_{^{86}Sr}}\right] \quad \text{(Equation 1)}$$

$$R_{sample,corrected}^{^{87}Sr/^{86}Sr} = \left(\frac{R_{std,true}^{^{87}Sr/^{86}Sr}}{\frac{R_{std-1,measured}^{^{87}Sr/^{86}Sr} + R_{std+1,measured}^{^{87}Sr/^{86}Sr}}{2}}\right) x \, R_{sample,measured}^{^{87}Sr/^{86}Sr} \quad \text{(Equation 2)}$$

where $m^{86,87,88}Sr$ are the atomic masses of the isotopes of interest and f is the mass bias correction factor. It has to be stressed that the $^{88}Sr/^{86}Sr$ isotope ratio is affected by natural isotope fractionation,[56] but the natural variation this gives rise to can be considered negligible within the precision attainable in this work. Furthermore, it has to be pointed out that no additional corrections were performed in this work (e.g., blank subtraction and/or mathematical equations for additional correction for spectral overlap), which further confirms the potential of the newly developed methodology for straightforward Sr isotopic analysis *via* LA-ICP-MS/MS.

3. RESULTS AND DISCUSSION

3.1. Optimization of conditions for Sr isotopic analysis of solid samples with high Rb/Sr ratio via LA-ICP-MS/MS

3.1.1. Use of chemical resolution to avoid spectral overlap

A mixture of CH_3F/He (1:9) was selected as the best suited reaction gas due to the high efficiency of the reaction with Sr – leading to the formation of SrF^+ ions – while Rb and Kr do not show reactivity towards CH_3F.[37] By using the capabilities provided by the MS/MS mode, all concomitant matrix ions with an m/z ratio different from that of the respective analyte ions, i.e., $^{86,87,88}Sr$, are removed by the first quadrupole (Q1), while the second quadrupole (Q2) is fixed at the m/z ratio of the new reaction product ions, i.e.,$^{86,87,88}SrF^+$ (see Figure 2). The CH_3F/He gas flow rate was optimized to obtain the maximum SrF^+ signal intensity, which was attained at 0.90 mL min^{-1}. The capabilities of the selected reaction gas mixture to overcome Sr/Rb isobaric overlap at m/z = 87 are documented in Figure 3, which represents the $^{87}Sr/^{86}Sr$ and $^{88}Sr/^{86}Sr$ isotope ratio results (left y-axis and right y-axis, respectively) as a function of the Rb/Sr ratio – for a set of 6 geological RMs in both, "vented" (no gas) and CH_3F/He mode. Within the precision attainable in this work, no significant differences were found between the $^{88}Sr/^{86}Sr$ isotope ratio results in both gas modes, which indicates absence of additional fractionation produced by collisions and/or reactions in the cell, in contrast with what was observed in a previous work carried out with a quadrupole-based reaction cell.[38] As expected, the $^{87}Sr/^{86}Sr$ isotope ratios become increasingly biased high with rising Rb/Sr ratio in "vented" mode due $^{87}Sr/^{87}Rb$ isobaric overlap. However, the use of 0.90 mL min^{-1} of CH_3F/He suffices to remove the isobaric interference of ^{87}Rb, thus potentially allowing direct Sr isotopic analysis of solid samples with high Rb/Sr ratio *via* LA-ICP-MS/MS. Additionally, the presence of He in the gas mixture might lead to an improvement of the isotope ratio precision by the so-called collisional damping effect,[57] while the slowdown of the ion beam also has a positive effect on the reaction efficiency due to an increase of the residence time of the ions in the cell.[41, 43]

3.1.2. Optimization of operational conditions

Isotopic analysis *via* LA-ICP-MS has been carried out in both "dry" and "wet" mode.[11] The use of "wet" plasma conditions, derived by the simultaneous introduction of an aqueous solution into the ICP, brings about several advantages. An internal standard can be admixed for mass bias correction, standard solutions can be introduced for calibration purposes and overall, a higher robustness, thus better signal stability, have been reported as a result of a lighter effect of the introduction of ablated material on the plasma stability.[58-60]

In this work, the carrier gas transporting the aerosol produced in the ablation process was introduced into the spray chamber, *via* the make-up gas inlet (see Figure 1b). No other changes to the introduction system are required, thus facilitating transition to PN-ICP-MS/MS for other applications in routine laboratories. Of course, it has to be stressed that the use of "wet" plasma conditions involves an increase in the level of oxide species, which might aggravate the accuracy for elements suffering from oxide-based polyatomic interferences.

For both introduction system approaches (see also Fig. 1), ablation conditions and data acquisition parameters were optimized in order to obtain the best transient signal stability – leading to the best internal precision – without compromising isotope ratio accuracy and/or sample throughput. NIST SRM 610 was the standard selected for optimization purposes due to its relatively high homogeneity. First, the influence of dwell time on the accuracy and precision of the Sr isotope ratios was assessed. The results obtained are presented in Figure 4A, which shows the RSD (%, left y-axis) and $^{87}Sr/^{86}Sr$ isotope ratio (right y-axis) as a function of dwell time (2 - 500 ms) for both "dry" (red) and "wet" (blue) modes. As can be seen, the RSD (%) improves clearly with the increase in dwell time until a constant value was reached at ~300 - 400 ms. The same trend was found for both plasma conditions, although better signal stability was achieved in "wet" mode, which as indicated above, can be attributed to the reduction of fluctuations in plasma load. To evaluate whether the improvement in precision observed under "wet" conditions, was truly owing to the wet plasma conditions and not merely to a change in sample aerosol trajectory, possibly affecting the particle size distribution, the "wet" setup was also assessed without co-nebulized water. The results obtained under these conditions show an RSD per replicate measurement of 2.50 ± 0.30 %, which is not significantly different from that obtained with the "dry" configuration, thus illustrating the added value of "wet" plasma

conditions. On the other hand, variation in the $^{87}Sr/^{86}Sr$ ratio was established at low dwell times, and only at values ≥300 ms, the ratio appears to have stabilized. This tendency was also observed in a previous work,[43] in which it was demonstrated that a wait time offset (WTO) of 5 ms suffices to stabilize the Sr isotope ratios at low dwell times. No such effect was observed for dwell times ≥300 ms. These observations can most probably be attributed to the additional time required for stable interaction between the ions and a reactive gas such as CH_3F in the cell. Based on these results, 300 ms was selected as dwell time and used throughout further work. It can also be seen from Figure 4A, that the raw $^{87}Sr/^{86}Sr$ isotope ratios (before mass bias correction) are clearly biased towards a higher value with respect to the reference value (recommended value for NIST SRM 610 = 0.709699 ± 0.000018[53]), even more in "dry" plasma conditions.[59]

Another important prerequisite for successful isotopic analysis is sufficient signal intensity (cf. counting statistics). Maximum sensitivity was found when using the instrument settings summarized in Table 2. The detector dead time was experimentally determined to be 32.6 ± 0.3 ns. In both modes, the signal intensity was varied by changing the laser beam diameter. Figure 4B shows how the RSD (%) per replicate measurement (the experiment was repeated 3 times) varies as a function of the laser beam diameter. The results further confirm a better precision in "wet" mode, and in general, it can be seen that for a laser beam diameter ≤20 μm (beam waist size, corresponding to ~5 x 10^5 counts/s for NIST SRM 610), the precision is degraded due to poor counting statistics. Thus, in further experiments, the laser beam diameter was adjusted such that for all standards and samples a ^{88}Sr signal intensity of approximately 6 x 10^5 cps was obtained (the system response for NIST SRM 610 using a laser beam diameter of 25 μm) as to prevent the dual-mode discrete dynode detector from switching between counting and analog mode.

Finally, the effect of different acquisition times on the signal stability (expressed as the RSD (%) per replicate measurement) was evaluated. The results are shown in Figure 4C, from which once more, it can be seen that the precision in "wet" mode is better than that in "dry" mode. The average RSD (%) values seem to stabilize for acquisition times ≥60 s, but the variation in RSD values obtained for different replicate measurements, is lower at higher acquisition times (Figure 4C). A compromise between precision and acquisition time was found at 60 s, although longer acquisition times can be

used to increase the final precision. It has to be taken into account that although 60 s of acquisition time was selected, differences in stabilization and washout time in "dry" and "wet" mode were present, leading to run times per replicate measurement of 65 and 75 s, respectively.

3.1.3. Figures of merit for Sr isotope ratio measurements via LA-ICP-MS/MS

Once the instrument settings and data acquisition parameters were optimized as indicated above, the figures of merit for Sr isotopic analysis were evaluated. The accuracy and precision of the approach developed was tested by means of the determination of the $^{87}Sr/^{86}Sr$ isotope ratio in NIST SRM 610. As explained in section 2.3, 12 replicate measurements were performed for each analysis, which was repeated 5 times in a standard-sample-standard sequence. NIST SRM 612 (laser beam diameter of 85 μm) was selected as external standard for mass discrimination correction purposes – double correction approach, after internal correction *via* the Russell law (see section 2.3 for a detailed explanation of the mass bias correction). Figure 5 represents the average value (black lines), internal precision (error bars) and external precision (black dashed lines) for the Sr isotope ratios in both "dry" and "wet" plasma modes. The green line indicates the reference value. Accurate results were obtained in both approaches, with $^{87}Sr/^{86}Sr$ isotope ratio values of 0.70945 ± 0.00121 and 0.70968 ± 0.00035 for "dry" and "wet" plasma conditions, respectively (recommended value = 0.709699 ± 0.000018,[53] green line in Figure 5). However, as was already expected from the conclusions drawn during optimization, the results obtained in "wet" plasma mode show a significant improvement in internal precision (expressed as within-run precision and defined as the standard deviation for 12 replicate measurements within a single analysis) and external precision (expressed as the standard deviation for 5 consecutive analyses). An internal precision in the range of 0.30 – 0.43 % (RSD) was achievable for "dry" and of 0.09 – 0.16 % (RSD) for "wet" conditions (~2.5-fold improvement for "wet" plasma mode). These values are in good agreement with those reported in the literature for LA-ICP-QMS,[11] and similar to the isotope ratio precision attained using ICP-MS/MS for liquid/digested samples.[43] Once again, it was verified whether the "wet" plasma conditions rather than the different trajectory followed by the sample aerosol were at the origin of the improvement in precision observed. The "wet" setup was also assessed without co-nebulized water. Under these conditions, the RSD (0.31%) obtained is not

significantly different from that obtained using the "dry" approach (0.30 – 0.43 %), demonstrating that the improvement in precision can be attributed to "wet" plasma conditions.

External precision values of 0.17 and 0.05 % RSD were obtained for “dry” and “wet” plasma modes, respectively (~3-fold improvement for “wet” plasma mode). It has to be pointed out that accurate and precise results were obtained in spite of the high Rb/Sr ratio in NIST SRM 610 and 612 (~0.82 and 0.40, respectively), and the differences in Sr concentration between both materials (78.4 ± 0.2 and 515.5 ± 1 μg g^{-1}, respectively). Based on those results, LA-ICP-MS/MS operated under “wet” plasma conditions was selected as the more suitable approach and was used throughout the further work.

3.2. Proof-of-concept: Sr isotopic analysis of geological RMs

The same protocol for Sr isotopic analysis *via* LA-ICP-MS/MS under “wet” plasma conditions was applied to 7 geological RMs. This selection of RMs has been made in order to be able to demonstrate the capabilities of the approach developed for a wide range of (i) Rb/Sr ratio, (ii) matrix composition and (iii) Sr concentration (see Table 1 and 3). NIST SRM 610 was used as the external standard for mass bias correction purposes. The results are summarized in Table 3. No significant differences were found between the $^{87}Sr/^{86}Sr$ ratios obtained in this work and the corresponding literature values, even for those materials with high Rb/Sr ratio (total range in materials studied: 0.02 – 0.82). In addition, from the comparison with the results obtained in section 3.1.3 for NIST SRM 610, the attainable precision does not seem to be affected by the matrix, and external precision values in the range of 0.024 – 0.054 % RSD (n = 5) are reported in Table 3. It is very important to note that no further sample/standard matrix-matching was required despite the differences in matrix composition (see Table 1). Also, no additional correction for remaining spectral overlap was required. Therefore, these results further illustrate the capabilities of the approach developed for accurate and precise Sr isotopic analysis of solid samples with high Rb/Sr ratio *via* LA-ICP-MS/MS.

4. CONCLUSION

For the first time ever (to the best of the authors’ knowledge), this work reports on the direct Sr isotopic analysis of solid samples with high Rb/Sr ratio by means of a combination of laser ablation and tandem ICP – mass spectrometry. The use of chemical resolution – using 0.90 mL min^{-1} of a

CH_3F/He mixture as reaction gas – in a LA-ICP-MS/MS system operated under "wet" plasma conditions, suffices to overcome $^{87}Sr/^{87}Rb$ isobaric overlap and to obtain accurate and precise (~0.05% RSD, external precision) isotope ratio results, independent of the matrix composition, Sr concentration and/or Rb/Sr ratio within the range of materials studied. Instrumental mass discrimination was corrected for by a combination of internal correction relying on the Russell law, followed by external correction in an SSB approach. One glass CRM (NIST SRM 610) was used as external standard for all geological RMs investigated – no closer matrix-matching or additional correction for remaining spectral overlap was required. The straightforward methodology developed in this work is a real alternative for the more common approaches dealing with Sr isotopic analysis, and the results obtained suggest its applicability in many real-life applications in routine laboratories, e.g., for pre-selecting samples for subsequent higher-precision isotopic analysis *via* TIMS or MC-ICP-MS.

ACKNOWLEDGMENTS

The UGent authors acknowledge Agilent Technologies for providing them with an ACT-UR research project grant, the Special Research Fund of Ghent University (BOF-UGent) for providing research funding and Teledyne Cetac Technologies for financial support for their LA-ICP-MS research projects. SVM is a PhD fellow of the Flemish Research Foundation (FWO - Vlaanderen). MR acknowledges the funding from the Spanish Ministry of Economy and Competitiveness (Project CTQ2012-33494) and from the Aragón Government (Fondo Social Europeo). The authors thank Dr. Steven Goderis (VUB and UGent) for providing them with the USGS geochemical reference materials.

AUTHOR INFORMATION

Corresponding Author

Phone: +3292644848; E-mail: Frank.Vanhaecke@UGent.be

References

1. R. A. Bentley, *J. Archaeol. Method Th.*, 2006, **13**, 135 - 187.
2. W. Neumann and E. Huster, *Earth Planet. Sci. Lett.*, 1976, **33**, 277 - 288.
3. F. Begemann, K. R. Ludwig, G. W. Lugmair, K. Min, L. E. Nyquist, P. J. Patchett, P. R. Renne, C.-Y. Shih, I. M. Villa and R. J. Walker, *Geochim. Cosmochim. Acta*, 2001, **65**, 111 - 121.
4. F. Vanhaecke, L. Balcaen and D. Malinovsky, *J. Anal. At. Spectrom.*, 2009, **24**, 863 - 886.
5. L. Font, G. van der Peijl, I. v. Wetten, P. Vroon, B. van der Wagt and G. DAvies, *J. Anal. At. Spectrom.*, 2012, **27**, 719 - 732.
6. F. Vanhaecke and L. Moens, *Anal. Bioanal. Chem.*, 2004, **378**, 232 - 240.
7. P. Cheng, G. K. Koyanagi and D. K. Bohme, *Anal. Chim. Acta*, 2008, **627**, 148 - 153.
8. C. B. Douthitt, *Anal. Bioanal. Chem.*, 2008, **390**, 437 - 440.
9. F. Vanhaecke, G. D. Wannemacker, L. Moens and J. Hertogen, *J. Anal. At. Spectrom.*, 1999, **14**, 1691 - 1696.
10. C. M. Almeida and M. T. S. D. Vasconcelos, *J. Anal. At. Spectrom.*, 2001, **16**, 607 - 611.
11. M. Aramendía, M. Resano and F. Vanhaecke, *J. Anal. At. Spectrom.*, 2010, **25**, 390 - 404.
12. S. R. Copeland, M. Sponheimer, P. J. L. Roux, V. Grimes, J. A. Lee-Thorp, D. J. de Ruiter and M. P. Richards, *Rapid. Commun. Mass Spectrom.*, 2008, **22**, 3187 - 3194.
13. J. S. Becker, *J. Anal. At. Spectrom.*, 2002, **17**, 1172 - 1185.
14. B. Hattendorf, C. Latkoczy and D. Günther, *Anal. Chem.*, 2003, 341A - 347A.
15. M. Resano, E. García-Ruiz and F. Vanhaecke, *Mass Spectrom. Rev.*, 2010, **29**, 55 - 78.
16. R. E. Russo, X. Mao, J. J. Gonzalez, V. Zorba and J. Yoo, *Anal. Chem.*, 2013, **85**, 6162 - 6177.
17. T. Waight, J. Baker and D. Peate, *Int. J. Mass Spectrom.*, 2002, **221**, 229 - 244.
18. A. Simonetti, M. R. Buzon and R. A. Creaser, *Archaeometry*, 2008, **2**, 371 - 385.
19. F. C. Ramos, J. A. Wolff and D. L. Tollstrup, *Chem. Geol.*, 2004, **211**, 135 - 158.
20. P. Galler, A. Limbeck, S. F. Boulyga, G. Stingeder, T. Hirata and T. Prohaska, *Anal. Chem.*, 2007, **79**, 5023 - 5029.

21. D. D. Muynck, G. Huelga-Suarez, L. Van Heghe, P. Degryse and F. Vanhaecke, *J. Anal. At. Spectrom.*, 2009, **24**, 1498 - 1510.

22. S. J. Romaniello, M. P. Field, H. B. Smith, G. W. Gordon, M. H. Kim and A. D. Anbar, *J. Anal. At. Spectrom.*, 2015, **DOI: 10.1039/c5ja00205b**.

23. F. Vanhaecke, L. Moens, R. Dams, I. Papadakis and P. Taylor, *Anal. Chem.*, 1997, **69**, 268 - 273.

24. N. Jakubowski, L. Moens and F. Vanhaecke, *Spectrochim. Acta, Part B*, 1998, **53**, 1739 - 1763.

25. L. Moens and N. Jakubowski, *Anal. Chem.* , 1998, **70**, 251A - 256A.

26. J. N. Christensen, A. N. Halliday, D.-C. Lee and C. M. Hall, *Earth Planet. Sci. Lett.*, 1995, **136**, 79 - 85.

27. J. Davidson, F. Tepley III, Z. Palacz and S. Meffan-Main, *Earth Planet. Sci. Lett.*, 2001, **184**, 427 - 442.

28. K. P. Jochum, B. Stoll, U. Weis, D. V. Kuzmin and A. V. Sobolev, *J. Anal. At. Spectrom*, 2009, **24**, 1237 - 1243.

29. L. Balcaen, I. D. Schrijver, L. Moens and F. Vanhaecke, *Int. J. Mass Spectrom.*, 2005, **242**, 251 - 255.

30. P. Z. Vroon, B. van der Wagt, J. M. Koornneef and G. R. Davies, *Anal. Bioanal. Chem.*, 2008, **390**, 465 - 476.

31. P. Rodríguez-González, J. M. Marchante-Gayón, J. I. García Alonso and A. Sanz-Medel, *Spectrochim. Acta, Part B*, 2005, **60**, 151 - 207.

32. S. A. Crowe, B. J. Fryer, I. M. Samson and J. E. Gagnon, *J. Anal. At. Spectrom.*, 2003, **18**, 1331 - 1338.

33. P. P. Coetzee and F. Vanhaecke, *Anal. Bioanal. Chem*, 2005, **383**, 977 - 984.

34. S. D. Tanner and V. I. Baranov, *J. Am. Soc. Mass Spectrom.*, 1999, **10**, 1083 - 1094.

35. S. D. Tanner, V. I. Baranov and D. R. Bandura, *Spectrochim. Acta, Part B*, 2002, **57**, 1361 - 3452.

36. J. J. Sloth and E. H. Larsen, *J. Anal. At. Spectrom.*, 2000, **15**, 669 - 672.

37. L. J. Moens, F. F. Vanhaecke, D. R. Bandura, V. I. Baranov and S. D. Tanner, *J. Anal. At. Spectrom.*, 2001, **16**, 991 - 994.

38. F. Vanhaecke, L. Balcaen, I. Deconinck, I. D. Schrijver, C. M. Almeida and L. Moens, *J. Anal. At. Spectrom.*, 2003, **18**, 1060 - 1065.

39. M. Resano, P. Marzo, M. Pérez-Arantegui, M. Aramendía, C. Cloquet and F. Vanhaecke, *J. Anal. At. Spectrom.*, 2008, **23**, 1182 - 1191.

40. L. Balcaen, E. Bolea-Fernandez, M. Resano and F. Vanhaecke, *Anal. Chim. Acta*, 2015, DOI: 10.1016/j.aca.2015.08.053.

41. E. Bolea-Fernandez, L. Balcaen, M. Resano and F. Vanhaecke, *Anal. Chem.*, 2014, **86**, 7969 - 7977.

42. E. Bolea-Fernandez, L. Balcaen, M. Resano and F. Vanhaecke, *Anal. Bioanal. Chem.*, 2015, **407**, 919 - 929.

43. E. Bolea-Fernandez, L. Balcaen, M. Resano and F. Vanhaecke, *J. Anal. At. Spectrom.*, 2015, DOI: 10.1039/c5ja00157a.

44. S. Díaz Fernández, N. Sigishama, J. R. Encinar and A. Sanz-Medel, *Anal. Chem.*, 2012, **84**, 5851 - 5857.

45. L. Balcaen, E. Bolea-Fernandez, M. Resano and F. Vanhaecke, *Anal. Chim. Acta*, 2014, **809**, 1 - 8.

46. C. D. B. Amaral, R. S. Amais, L. L. Fialho, D. Schiavo, T. Amorim, A. R. A. Nogueira, F. R. P. Rocha and J. A. Nóbrega, *Anal. Methods*, 2015, **7**, 1215 - 1220.

47. L. Balcaen, G. Woods, M. Resano and F. Vanhaecke, *J. Anal. At. Spectrom.*, 2013, **28**, 33 - 39.

48. M. Tanimizu, N. Sugiyama, E. Ponzevera and G. Bayon, *J. Anal. At. Spectrom.*, 2013, **28**, 1372 - 1376.

49. J. Zheng, W. Bu, K. Tagami, Y. Shikamori, K. Nakano, S. Uchida and N. Ishii, *Anal. Chem.*, 2014, **86**, 7103 - 7110.

50. T. Ohno and Y. Muramatsu, *J. Anal. At. Spectrom.*, 2014, **29**, 347 - 351.

51. D. P. Bishop, D. Clases, f. Fryer, E. Williams, S. Wilkins, D. J. Hare, N. Cole, U. Karst and P. A. Doble, *J. Anal. At. Spectrom*, 2015, **DOI: 10.1039/c5ja00293a**.

52. N. J. G. Pearce, W. T. Perkins, J. A. Westgate, M. P. Gorton, S. E. Jackson, C. R. Neal and S. P. Chenery, *Geostand. Newsl.*, 1996, **21**, 115 - 144.

53. GeoReM, http://georem.mpch-mainz.gwdg.de (accessed September 2015).

54. GERM Reservoir Database, http://earthref.org/GERMRD (accessed October 2015).

55. L. Yang, *Mass Spectrom Rev.*, 2009, **28**, 990 - 1011.

56. J. Irrgeher, T. Prohaska, R. E. Sturgeon, Z. Mester and L. Yang, *Anal. Methods*, 2013, **5**, 1687 - 1694.

57. D. R. Bandura, V. I. Baranov and S. D. Tanner, *J. Anal. At. Spectrom.*, 2000, **15**, 921 - 928.

58. C. O'Connor, B. L. Sharp and P. Evans, *J. Anal. At. Spectrom*, 2006, **21**, 556 - 565.

59. M. Resano, M. P. Marzo, R. Alloza, C. Saéz, F. Vanhaecke, L. Yang, S. Willie and R. E. Sturgeon, *Anal. Chim. Acta*, 2010, **677**, 55 - 63.

60. M. R. Flórez, M. Aramendía, M. Resano, A. C. Lapeña, L. Balcaen and F. Vanhaecke, *J. Anal. At. Spectrom.*, 2013, **28**, 1005 - 1015.

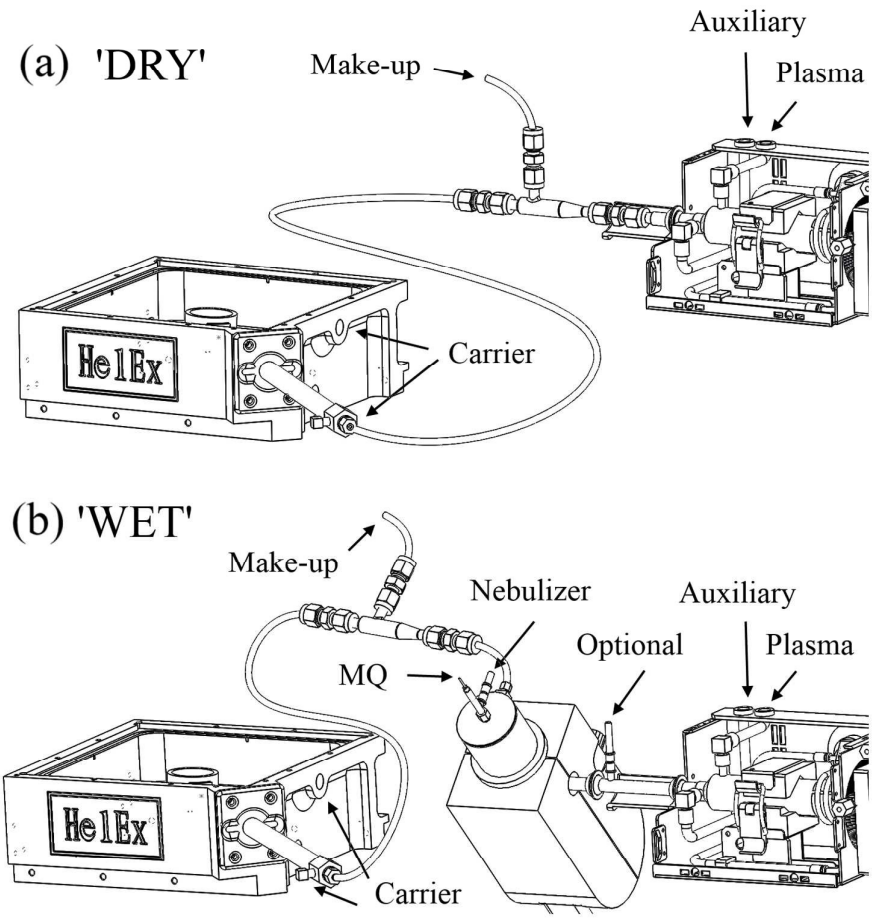

Figure 1. Graphic representation of the sample introduction set-ups and their gas flows for "dry" (a) and "wet" (b) plasma conditions

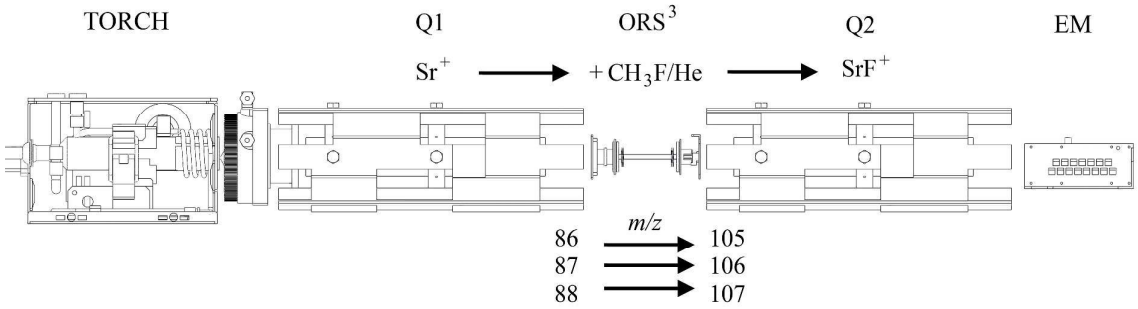

Figure 2. Schematic representation of the operating principle of tandem ICP–MS for interference-free Sr isotopic analysis *via* conversion of Sr into SrF^+. Q1 and Q2 represent the first and second quadrupole, while ORS^3 and EM are the acronyms for the type of collision-reaction cell (octopole reaction system 3rd generation), and detector (electron multiplier), respectively.

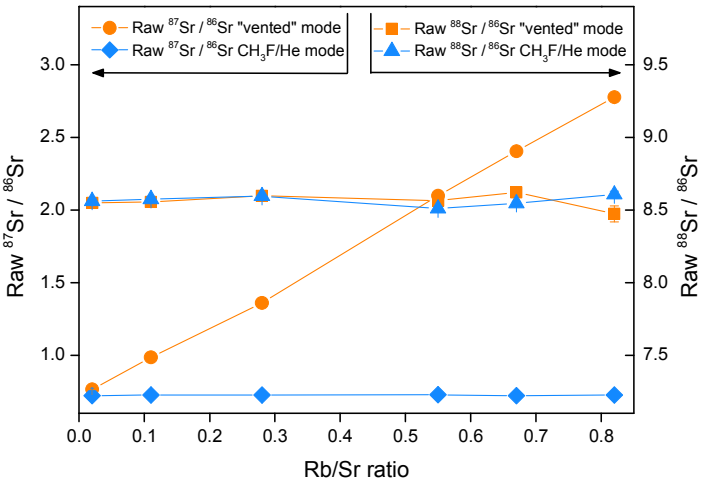

Figure 3. Influence of the Rb/Sr ratio on the raw $^{87}Sr/^{86}Sr$ (left y-axis) and $^{88}Sr/^{86}Sr$ (right y-axis) isotope ratios for "vented" (orange) and CH_3F/He (blue) modes

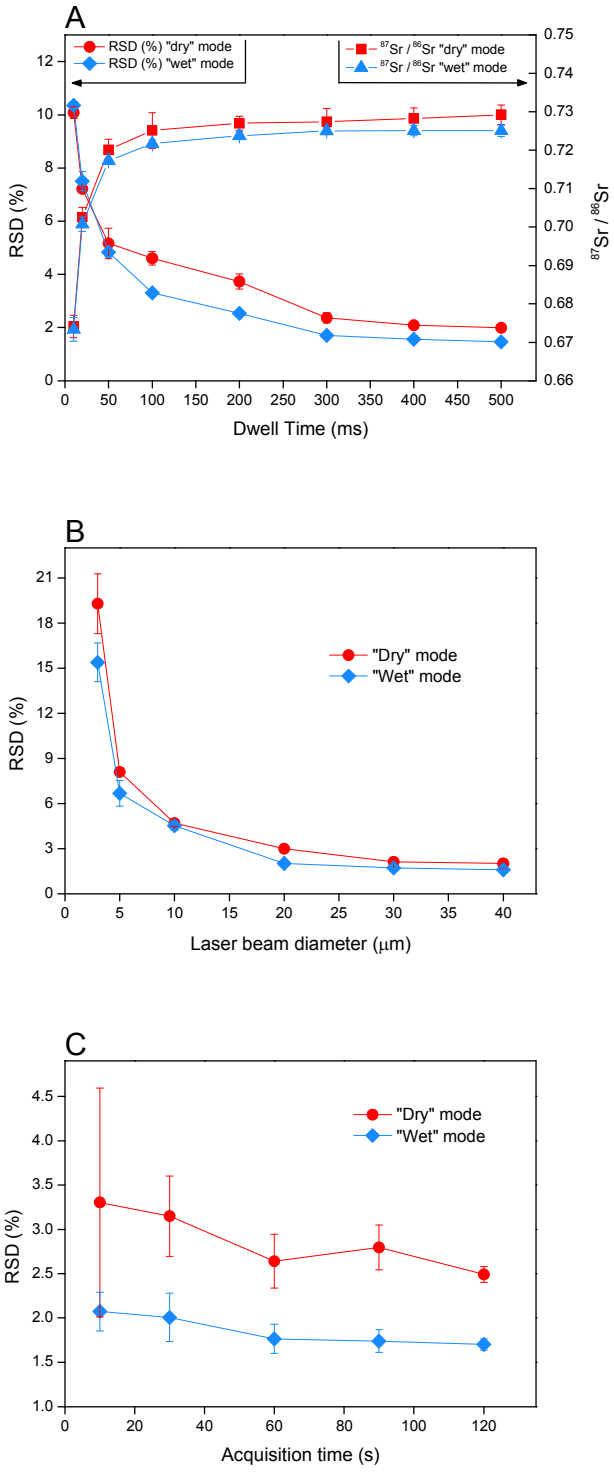

Figure 4. (A) RSD (%) – left y-axis – and $^{87}Sr/^{86}Sr$ isotope ratio – right y-axis – as a function of the dwell time in both "dry" (red) and "wet" (blue) conditions. **(B)** RSD (%) per replicate measurement as a function of laser beam diameter (μm) using NIST SRM 610 in both "dry" and "wet" conditions. **(C)** RSD (%) per replicate measurement as a function of acquisition time (s) for NIST SRM 610 analyzed in both "dry" and "wet" conditions. In all figures, each point corresponds with the average and standard deviation of 3 replicate measurements.

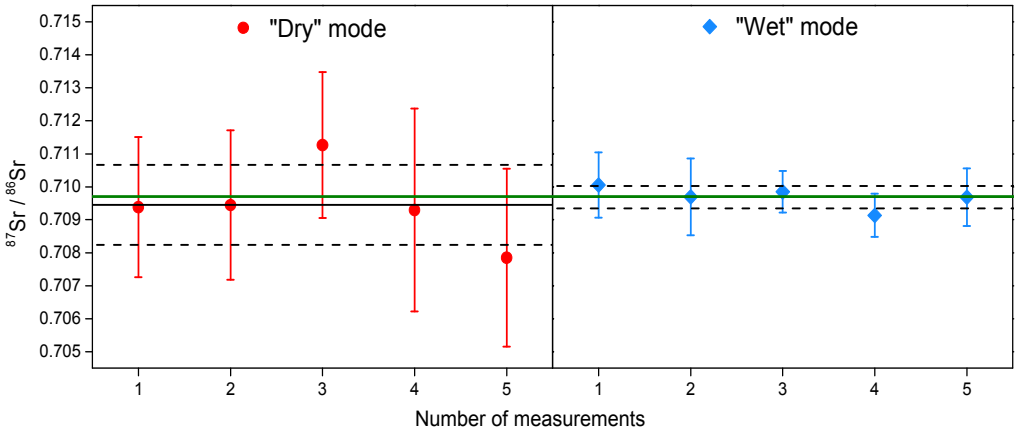

Figure 5. $^{87}Sr/^{86}Sr$ isotope ratio results obtained for NIST SRM 610 after double mass bias correction (Russell law followed by SSB using NIST SRM 612 as external standard) upon 5 replicate analyses in both "dry" and "wet" conditions. The error bars indicate the standard deviation of 12 replicate measurements (within-run precision). The black and dashed lines correspond with, respectively, the average and standard deviation (external precision) of 5 replicate analyses. The green line represents the recommended $^{87}Sr/^{86}Sr$ isotope ratio for NIST SRM 610.[53]

Table 1. Chemical composition of the reference materials (RMs) used in this work [52, 53]

Reference Material	Type	Sr ($\mu g\ g^{-1}$)	Rb ($\mu g\ g^{-1}$)	Al_2O_3 (% m/m)	CaO (% m/m)	FeO (% m/m)	K_2O (% m/m)	MgO (% m/m)	MnO (% m/m)	Na_2O (% m/m)	SiO_2 (% m/m)
NIST SRM 610	Silicate	515.5 ± 1	425.7 ± 1	2.039 ± 0.157	11.45 ± 0.231	0.056 ± 0.016	0.059 ± 0.002	0.065 ± 0.004	0.054 ± 0.005	13.352 ± 0.681	69.975 ± 0.391
NIST SRM 612	Silicate	78.4 ± 0.2	31.4 ± 0.4	2.11 ± 0.16	11.93 ± 0.22	0.02 ± 0.00	0.01 ± 0.00	0.00	0.01 ± 0.00	13.98 ± 0.56	71.90 ± 0.96
USGS BHVO-2G	Basalt	396 ± 1	9.2 ± 0.04	13.6 ± 0.1	11.4 ± 0.1	11.3 ± 0.1	0.51 ± 0.02	7.13 ± 0.02	0.17 ± 0.03	2.4 ± 0.1	49.3 ± 0.1
USGS NKT-1G	Nephelinite	1195 ± 57	30.7 ± 1.25	10.5	13.4	12.2	1.27	14.2	0.24	3.85	38.9
USGS TB-1G	Basalt	1352 ± 6	142 ± 0.5	17.12	6.7	8.67	4.52	3.51	0.18	3.56	54.29
USGS BCR-2G	Basalt	342 ± 4	47 ± 0.5	13.4 ± 0.4	7.06 ± 0.11	12.4 ± 0.3	1.74 ± 0.04	3.56 ± 0.09	0.19 ± 0.01	3.23 ± 0.07	54.4 ± 0.4
MPI-DING T1-G	Diorite	284 ± 6	79.7 ± 3.5	17.1 ± 0.2	7.1 ± 0.09	6.44 ± 0.06	1.96 ± 0.04	3.75 ± 0.04	0.127 ± 0.006	3.13 ± 0.09	58.6 ± 0.4
USGS GSD-1G	Basalt	69.4 ± 0.7	37.3 ± 0.4	13.4 ± 0.3	7.2 ± 0.1	13.3 ± 0.1	3 ± 0.1	3.6 ± 0.04	---	3.6 ± 0.2	53.2 ± 0.8
MPI-DING ATHO-G	Rhyolite	94.1 ± 2.7	65.3 ± 3	12.2 ± 0.02	1.7 ±0.03	3.27 ± 0.1	2.64 ± 0.09	0.103 ± 0.01	0.106 ± 0.005	3.75 ± 0.31	75.6 ± 0.7

Table 2. Instrument settings and data acquisition parameters for Sr isotopic analysis using LA-ICP-MS/MS in both "dry" and "wet" conditions

	"Dry" conditions	"Wet" conditions
Analyte G2 laser ablation system		
Energy density (J cm^{-2})	3.54	
Repetition rate (Hz)	40	
Scan speed (μm s^{-1})	15	
Beam waist diameter (μm)	20 – 85	
He carrier gas (L min^{-1})	0.42	
Agilent 8800 ICP-MS/MS		
Scan type	MS/MS	
RF power (W)	1550	
Sample depth (mm)	4.5	3.5
Ar plasma gas flow rate (L min^{-1})	15	
Ar auxiliary gas flow rate (L min^{-1})	0.90	
Ar nebulizer gas flow rate (L min^{-1})	---	1
Ar make-up gas (L min^{-1})	0.9	0.33
Water uptake rate (mL min^{-1})	---	0.30
Spray chamber temperature (°C)	---	2
CH_3F/He gas flow rate (mL min^{-1})	0.90	
Q1 → Q2 masses	86 → 105 87 → 106 88 → 107	
Energy discrimination (V)	-8.4	
Wait time offset (s)	0	
Acquisition parameters		
Dwell time per acquisition point (ms)	300	
Acquisition time per replicate measurement (s)	60	
Run time per replicate measurement (s)	60	75
Number of replicate measurements	12	
Total analysis time per sample (min)	13.55	15.55
Detector dead time (ns)	32.6 ± 0.3	

Table 3. Results obtained upon Sr isotopic analysis *via* LA-ICP-MS/MS

Reference Material	Type	Laser beam diameter (μm)	Rb/ Sr ratio	Experimental $^{87}Sr/^{86}Sr$	RSD (%)	Recommended $^{87}Sr/^{86}Sr$[53]
USGS BHVO-2G	Basalt	30	0.02	0.70351 ± 0.00034	0.048	0.703469 ± 0.000007
USGS NKT-1G	Nephelinite	25	0.03	0.70363 ± 0.00017	0.024	0.703509 ± 0.000019
USGS TB-1G	Basalt	20	0.11	0.70576 ± 0.00030	0.042	0.705580 ± 0.000023
USGS BCR-2G	Basalt	30	0.14	0.70486 ± 0.00038	0.054	0.705003 ± 0.000004
MPI-DING T1-G	Diorite	40	0.28	0.70990 ± 0.00035	0.049	0.710093 ± 0.000017
USGS GSD-1G	Basalt	85	0.55	0.70924 ± 0.00029	0.040	0.709416 ± 0.000050
MPI-DING ATHO-G	Rhyolite	65	0.67	0.70310 ± 0.00026	0.036	0.703271 ± 0.000015